School of Pharmaceutical Engineering, Shenyang Pharmaceutical University, Shenyang, China

Application of novel pH sensitive isoniazid–heptamethine carbocyanine dye conjugates against prostate cancer cells

Xiao-Guang Yang[1], Yan-Feng Li[1], Yan-Jun Wang[1], Rui-Heng Kong[1], Dun Wang[1,*]

Received May 2020, accepted June 12, 2020

**Corresponding author: Dun Wang, School of Pharmaceutical Engineering, Shenyang Pharmaceutical University, Shenyang 110016, China*
wangduncn@hotmail.com

Pharmazie 75: 412-416 (2020) *doi: 10.1691/ph.2020.0521*

Recent studies have shown that monoamine oxidase A (MAOA) is significantly expressed in malignant prostate cancer (PCa) and plays an important role in tumorigenesis indicating its potential to serve as a target for PCa treatment. Here, we choose the small molecule isoniazid as the MAOA inhibition functionality and incorporated it in the tumor-targeting moiety of heptamethine carbocyanine dyes *via* a pH sensitive hydrazone bond to design and synthesize novel MAOA inhibitor isoniazid-heptamethine carbocyanine dye conjugates. Cytotoxicity assay in PC-3 cells shows that all conjugates possessed improved antitumor efficacy compared with isoniazid. The tested compounds also demonstrated a moderate MAOA inhibitory effect. In conclusion, these results indicate that these conjugates exert antitumor effects by delivering the MAOA-inhibiting moiety to PCa cells.

1. Introduction

Prostate cancer (PCa) has become the second leading cause of cancer deaths among Western males due to the growing of the elderly population. Current approaches to the treatment of early stage PCa include endocrine treatment, radiotherapy and surgical resection. However, these treatments are not suitable for the treatment of advanced malignant PCa (Aggarwal et al. 2011; Heidegger et al. 2013; Kgatle et al. 2016; Stavridi et al. 2010). Hence, there is an urgent need to better understand the mechanism of PCa progression and explore new targets in PCa.

A mitochondrial outer membrane enzyme, monoamine oxidase A (MAOA), regulates the monoamine neurotransmitter level in the body by oxidative deamination. The critical role of MAOA in maintaining neurotransmitter balance for brain function has long been recognized (Jolene et al. 2015; Shih et al. 1999; Wu et al. 1993; Sandi et al. 2015). Nevertheless, MAOA is suggested to play an important role in tumorigenesis (Sun et al. 2017; Liu et al. 2017; Li et al. 2017; Schwartz 2013). The process of oxidative deamination is accompanied by the generation of hydrogen peroxide (H_2O_2) belonging to the reactive oxygen species (ROS), which may cause cell damage and promote tumorigenesis and tumor development. Recently, a close correlation between high MAOA expression and PCa progression and poor prognosis of patients was revealed (Wu et al. 2014; True et al. 2006). Conversely, specific inhibition of MAOA suppresses the proliferation of PCa cells and the growth of tumor xenografts (Wu et al. 2014; Flam et al. 2010; Zhao et al. 2009). The growth and metastasis of PCa xenograft in which the MAOA gene has been knocked out was even reduced and eliminated (Liao et al. 2018; Xu et al. 2015; Wu et al. 2015). Further studies have shown MAOA to enhance the growth, invasion and metastasis of PCa cells by stabilizing the transcription factor HIF1α as a result of the elevation of ROS and inducing epithelial-mesenchymal transition (EMT) (True et al. 2006; Pheel et al. 2008; Wu et al. 2014). Above findings demonstrate the vital function of MAOA in PCa pathogenesis and suggest that MAOA may serve as a potential target for PCa treatment.

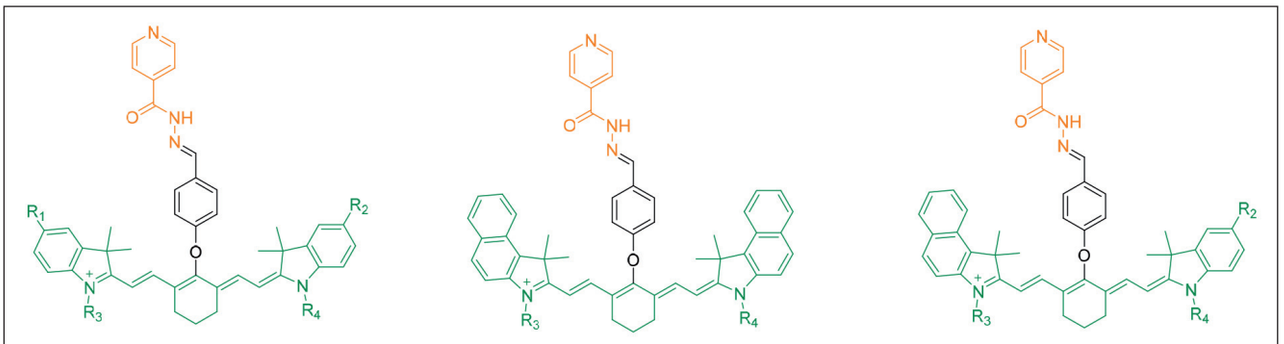

Z1: R_1=R_2=H, R_3=$(CH_2)_4SO_3^-$, R_4=$(CH_2)_4SO_3Na$
Z2: R_1=R_2=H, R_3=R_4=$(CH_2)_5COOH$
Z3: R_1=R_2=CH_3, R_3=R_4=$(CH_2)_5COOH$
Z5: R_1=R_2=OCH_3, R_3=$(CH_2)_4SO_3^-$, R_4=$(CH_2)_4SO_3Na$
Z6: R_1=R_2=CH_3, R_3=$(CH_2)_4SO_3^-$, R_4=$(CH_2)_4SO_3Na$
Z7: R_1=R_2=Br, R_3=R_4=$(CH_2)_5COOH$
Z9: R_1=H,R_2=Br, R_3=R_4=$(CH_2)_5COOH$

Z4: R_3=$(CH_2)_4SO3^-$, R_4=$(CH_2)_4SO_3Na$

Z8: R_2=H, R_3=$(CH_2)_4SO_3^-$, R_4=$(CH_2)_4SO_3Na$
Z10: R_2=CH_3, R_3=$(CH_2)_4SO_3^-$, R_4=$(CH_2)_4SO_3Na$

Fig. 1: Structures of designed compounds.

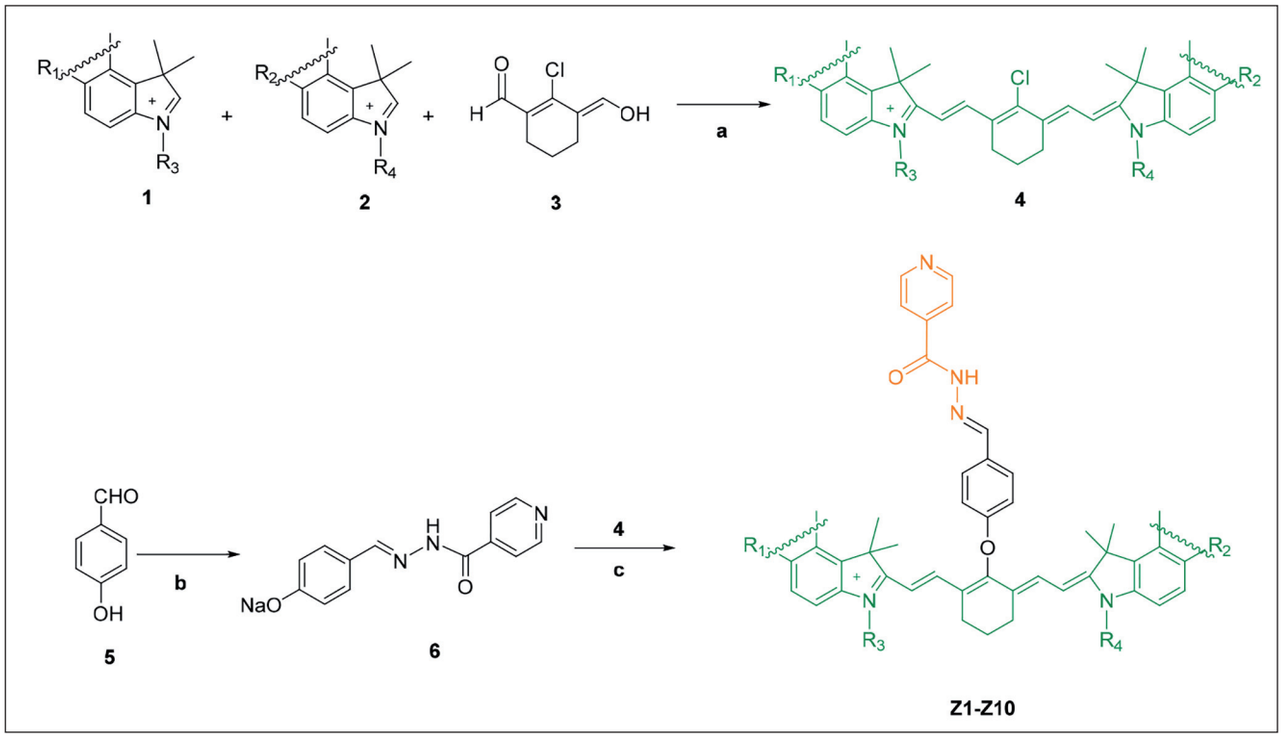

Fig. 2: Synthesis of designed compounds Z1-Z10. Reagents and conditions: (a) AcONa, C_2H_5OH, 60 °C; (b) NaH, THF, r.t.; isoniazid, CH_3OH, r.t.; (c) intermediate **4**, DMSO, r.t.

Given these results, we herein chose isoniazid, a small molecule hydrazine inhibitor of MAOA, which is an anti-tuberculosis drug. Considering the fact that MAOA is present in the central nervous system and other peripheral tissues, we integrated near-infrared (NIR) heptamethine carbocyanine dyes into the moiety of isoniazid for tumor targeting in order to achieve tumor-selectivity and reduce side effects.

The selective uptake of NIR heptamethine carbocyanine dyes into several types of cancer including PCa has been demonstrated. They could preferentially accumulate and retain in cancer cells but not in normal cells (Yang et al. 2010; Xiao et al. 2013). The mechanism of preferential uptake of NIR carbocyanine dyes into tumors are hypoxia inducible factor 1α/organic anion-transporting polypeptides (HIF1α/OATPs) signaling axis and higher negative mitochondrial transmembrane potentials in tumor cells (Khemthongcharoen et al. 2013; Shi et al. 2014; Luo et al. 2013; Henary et al. 2012; Wu et al. 2014; Hong et al. 2017; Tan et al. 2012; Luo et al. 2011; Sevick-Muraca et al. 2012; Lv et al. 2012; Lv et al. 2018; Wang et al. 1995). In this study, we designed and synthesized tumor-specific conjugates where tumor-targeting NIR heptamethine carbocyanine dyes were covalently bound to isoniazid *via* a hydrazone bond (Fig. 1). Their cytotoxicity against PC-3 cells was investigated and MAOA inhibitory activity was also evaluated.

2. Investigations and results

2.1. Synthesis

The synthetic route for compounds **Z1**-**Z10** is illustrated in Fig. 2. Substituted indoles **1** and **2** which could be the same or not and were both prepared by quaternization reaction described in our previous study (Yang et al. 2019) reacted with 2-chloro-3-(hydroxymethylene)cyclohex-1-enecarbaldehyde (**3**) in the presence of sodium acetate to afford intermediate **4**. *p*-Hydroxybenzenecarbaldehyde (**5**) was converted into its sodium salt by treatment with sodium hydride, the corresponding salt condensed with isoniazid and intermediate **6** was thus formed. The production of compounds **Z1**-**Z10** were carried out between intermediates **4** and **6** *via* substitution reaction.

2.2. Cytotoxicity evaluation

Cytotoxicity of the synthesized conjugates was evaluated by MTT assay in human PC-3 cells. Doxorubicin (DOX) was used as positive control. IC_{50} values of compounds Z1-Z10 against PC-3 cells are shown below in Table 1.

Table: Cytotoxicity assay of compounds Z1-Z10 against PC-3 cells (IC_{50}, μM)

Compd.	R_1	R_2	R_3	R_4	IC_{50} (μM)
Z1	H	H	$(CH_2)_4SO_3^-$	$(CH_2)_4SO_3Na$	-
Z2	H	H	$(CH_2)_5COOH$	$(CH_2)_5COOH$	24.57
Z3	CH_3	CH_3	$(CH_2)_5COOH$	$(CH_2)_5COOH$	-
Z4	-	-	$(CH_2)_4SO_3^-$	$(CH_2)_4SO_3Na$	12.54
Z5	OCH_3	OCH_3	$(CH_2)_4SO_3^-$	$(CH_2)_4SO_3Na$	43.71
Z6	CH_3	CH_3	$(CH_2)_4SO_3^-$	$(CH_2)_4SO_3Na$	38.04
Z7	Br	Br	$(CH_2)_5COOH$	$(CH_2)_5COOH$	11.35
Z8	-	H	$(CH_2)_4SO_3^-$	$(CH_2)_4SO_3Na$	21.42
Z9	H	Br	$(CH_2)_5COOH$	$(CH_2)_5COOH$	16.02
Z10	-	CH_3	$(CH_2)_4SO_3^-$	$(CH_2)_4SO_3Na$	10.34
Isoniazid	-	-	-	-	>200
DOX	-	-	-	-	0.48

The cytotoxicity assay showed that isoniazid indicated no obvious cytotoxicity with IC_{50}>200 μM. By comparison, all compounds exhibited preferable antitumor efficacy with IC_{50} at the range of 10-45 μM. Evaluation of IC_{50} values revealed that conjugates possessed a 5-20 times higher potency in inhibiting PC-3 cells growth than their parent compound, isoniazid.

2.3. MAOA inhibitory activity

MAOA inhibitory effects of compounds **Z4**, **Z7, Z9** and **Z10** were investigated in a LNCaP cell line which possesses a detectably high expression level of MAOA (Xu et al. 2015; Wu et al. 2014). (Table 2).

Table 2: MAOA inhibitory activity of compounds in LNCaP cells (IC_{50}, nM).

Compd.	**Z4**	**Z7**	**Z9**	**Z10**	Isoniazid
IC_{50} (nM)	840.7	421.7	854.2	512.3	>1000

Experimental data indicated that with isoniazid for comparison, four conjugates showed a significant increase in MAOA inhibition efficacy. The result seems consistent with that of the cytotoxicity assay.

3. Discussion

As MAOA showed its potential as a therapeutic target of advanced PCa, finding a suitable MAOA inhibitor becomes more and more crucial. Isoniazid is one of the earliest hydrazine MAOA inhibitors and the first line antituberculotic. Based on the principle of conventional drug in new use, we regard isoniazid as a potential therapeutic drug for PCa treatment. However, isoniazid showed serious side effects due to the lack of selective tumor uptake. Hence, we combined isoniazid with heptamethine carbocyanine by hydrazone bond, which can transport isoniazid effectively to tumor tissue. Studies have shown that isoniazid hydrazone and N-acetylated derivatives are more efficient and less hepatotoxic than isoniazid because of the blockage of the terminal amino group of hydrazine (Oliveira et al. 2017; Pahontu et al. 2017; Vila-Vicosa et al. 2017). Apparently, these conjugates showed some antitumor activity according to the results of MTT assay. We reasoned moderately increased cytotoxicity of these conjugates may be attributed to including of heptamethine carbocyanine functionality in their structures which result in its selectivity toward PC-3 cells mediated by OATPs and finally accumulation in the mitochondria of PC-3 cells, disrupting the normal function of mitochondrial. The fact that isoniazid exhibited negligible cytotoxicity may be due its poor passive diffusion into PC-3 cells. Above results indicated that incorporating heptamethine cyanine dyes for tumor targeting with the moiety of isoniazid was conducive to augmentation of *in vitro* anti-tumor activity against PC-3. Besides, some conjugates also exhibited obvious MAOA inhibitory effect. Thus, the marked antitumor activity of heptamethine carbocyanine-isoniazid conjugates may be attributed to preferential accumulation of conjugates mediated by OATPs and increased MAOA inhibitory effect derived from N-acylation of terminal hydrazine group of isoniazid. In conclusions, through combination of MAOA inhibitor isoniazid and tumor-targeting heptamethine carbocyanine dyes, we obtained novel MAOA inhibitor-heptamethine carbocyanine dyes conjugates. Compared with isoniazid these conjugates demonstrated improved *in vitro* antitumor efficacy as well as better MAOA inhibitory activity suggesting their antitumor ability may derive from tumor targeting and MAOA inhibition. Strategy in this article may provide a new platform for future generation of human PCa therapeutics.

4. Experimental

4.1. Materials

All reagents and solvents were commercially available. Isoniazid and 1,4-butane sultone were purchased from Aladdin (Shanghai, China). 6-Bromohexanoic acid was purchased from Meryer (Shanghai, China). Thiazolyl blue tetrazolium bromide (MTT) and other MTT assay reagents were purchased from Sigma-Aldrich (St. Louis, MO, USA). Clorgyline was purchased from Bide Pharmatech Ltd. (Shanghai, China). PC-3 and LNCaP cells were obtained from the Cell Bank of the Chinese Academy of Sciences (Shanghai, China). All chemicals and reagents employed were of analytical or HPLC grade.

4.2. Cytotoxicity evaluation

Cytotoxicity evaluation of compounds **Z1**-**Z10** were determined in PC-3 cells by MTT assay. In brief, PC-3 cells were incubated in 96-well plates at a density of 3000 cells per well for one day. Next, these cells were treated with various concentrations of tested compounds, isoniazid or DOX and incubated for four days. Then, the plates were added 10 μl of MTT (5 mg/ml) solution and incubated for 4 h at 37 °C. Finally, the medium was replaced with 200 μL DMSO in order to make the formed formazan crystals dissolved. The absorbance was tested at 570 nm on a microplate reader (Synergy-HT, Bio Tek Instruments, Winooski, VT, USA).

4.3. MAOA inhibition activity assay

About 6×10^5 LNCaP cells were plated in a 10-mm dish with 10% FBS medium for 24 h. After that, 10 pM, 1 nM, 100 nM, 10 μM cells of the tested compounds, isoniazid or clorgyline were added and kept for 48 h. Finally, MAOA activities were examined by Cell MAOA Assay Kit (Shanghai Chen gong Biotechnology, CHN, Lot No: 1-201838-10) according to the instruction. The MAOA activity was determined based on the substrate p-tyramine level after treatment with MAOB inhibitor pargyline.

4.4. Synthesis

*4.4.1. 2-(2-((2-chloro-3-(2-(3,3-dimethyl-1,5-disubstituted-2H-indol-2-ylidene)ethylidene)-1-cyclohexen-1-yl)vinyl)-3,3-dimethyl-1,5-disubstituted-3H-indolium (**4**)*

To a round-bottomed flask equipped with a magnetic stirrer were added 3,3-dimethyl-1,5-disubstituted-3*H*-indole (**1,** 1.0 equiv), 3,3-dimethyl-1,5-disubstituted-3*H*-indole (**2,** 1.0 equiv), 2-chloro-3-(hydroxymethylene)cyclohex-1-enecarbaldehyde (**3,** 1.0 equiv) and ethanol. The above solution was added sodium acetate (1.0 equiv) at one time. The reaction was kept at 60 °C and stirred for 5 h and then poured into ice-water. The mixture was still stirred for 6 h. Finally, after filtered, the filter cake was washed with ether and gold solid intermediate **4** was obtained after drying in vacuum.

*4.4.2. Sodium 4-(2-isonicotinoylhydrazinyl)phenoxide (**6**)*

Dry THF (30 mL) and p-hydroxybenzaldehyde (**5**, 1.0 g, 8.19 mmol, 1.0 equiv) was added a 100 ml round-bottomed flask equipped with a magnetic stirrer. NaH (197 mg, 8.19 mol, 1.0 equiv) was added to the solution and the suspension thus formed was stirred at room temperature for 2 h. After filtration of the mixture, a brown solid was obtained which was then added to anhydrous methanol (30 ml) followed by addition of isoniazid (1.24 g, 9.01 mmol, 1.1 equiv). Condensation reaction was carried out at room temperature for 5 h. The reaction was filtered to yield **6** (2.0g, 93.3%).

*4.4.3. General procedure for the synthesis of compounds **Z1**-**Z10***

Intermediate **4** (1.0 equiv) together with intermediate **6** (1.2 equiv) were added to DMSO. The resultant solution was stirred at room temperature overnight and then poured into dry ether. The mixture was allowed to stand overnight and filtered. The crude material was purified by silica gel column (eluted with methylene dichloride/methanol 5:1) to yield the product.

Sodium, 2-(2-((2-(4-(2-isonicotinoylhydrazinyl)phenoxy)-3-(2-(3,3-dimethyl-1-(4-sulfonylbutyl)-2H-indol-2-ylidene)ethylidene)-1-cyclohexen-1-yl)vinyl)-3,3-dimethylindol-1-yl)butane-1-sulfonate (**Z1**). MS(ESI) m/z: 932.4 $[M-Na+2H]^+$; ^{1}H NMR (600 MHz, DMSO-d_6) δ 8.76 (d, J=5.7 Hz, 2H), 8.46 (s, 1H), 7.85-7.79 (m, 5H),7.77 (s, 1H), 7.49 (d, J=7.5 Hz, 2H), 7.40 (d, J=8.0 Hz, 2H), 7.35 (t, J=7.6 Hz, 2H), 7.28 (d, J=8.3 Hz, 1H), 7.18 (t, J=7.4 Hz, 2H), 6.26 (d, J=14.2 Hz, 2H), 4.14 (s, 4H), 2.75 (s, 4H), 1.96 (s, 3H), 1.76 (d, J=6.7 Hz, 5H), 1.72 (dd, J=13.3, 6.5 Hz, 5H), 1.60 (t, J=37.7 Hz, 2H), 1.27 (s, 12H); ^{13}C NMR (101 MHz, DMSO-d_6) δ 171.51, 161.82, 161.50, 160.90, 150.29, 149.55, 148.52, 142.01, 140.94, 140.52, 140.48, 129.66, 128.49, 128.31, 124.78, 122.34, 121.51, 121.31, 115.02, 111.34, 100.50, 50.67, 48.53, 43.59, 27.19, 26.02, 23.71, 22.48, 20.72.

2-(2-((2-(4-(2-Isonicotinoylhydrazinyl)phenoxy)-3-(2-(3,3-dimethyl-1-(5-carboxypentyl)-2H-indol-2-ylidene)ethylidene)-1-cyclohexen-1-yl)vinyl)-3,3-dimethyl-1-(5-carboxypentyl)-3H-indolium bromide (**Z2**). MS(ESI) m/z: 888.54 $[M-Br]^+$; ^{1}H NMR (600 MHz, CD_3OD) δ 8.75 (d, J = 6.0 Hz, 2H), 8.34 (d, J = 30.6 Hz, 1H), 7.98 (s, 1H), 7.95 (d, J = 8.9 Hz, 2H), 7.91 (d, J = 6.1 Hz, 2H), 7.71 (d, J = 8.6 Hz, 1H), 7.41-7.35 (m, 3H), 7.31-7.23 (m, 4H), 7.21 (t, J = 7.4 Hz, 2H), 6.86 (d, J = 8.7 Hz, 1H), 6.19 (d, J = 14.2 Hz, 1H), 4.11 (t, J = 7.5 Hz, 4H), 2.78 (t, J = 6.0 Hz, 3H), 2.63 (t, J = 6.0 Hz, 1H), 2.19 (q, J = 7.5 Hz, 4H), 2.11-2.07 (m, 1H), 1.83 (dq, J = 22.7, 7.6 Hz, 4H), 1.73 (s, 3H), 1.68 (dt, J = 14.9, 7.4 Hz, 4H), 1.48 (dq, J = 22.4, 7.6 Hz, 4H), 1.37 (s, 8H), 1.35-1.28 (m, 4H); ^{13}C NMR (101 MHz, CD_3OD) δ 182.41, 173.67, 164.60, 164.49, 163.16, 151.10, 150.90, 143.61, 142.96, 142.53, 142.48, 131.48, 129.93, 129.78, 126.21, 123.35, 123.20, 122.92, 116.45, 112.12, 101.23, 50.30, 49.85, 49.71, 49.64, 49.50, 49.43, 49.28, 49.21, 49.07, 49.00, 48.79, 48.57, 48.36, 45.11, 38.84, 28.17, 27.89, 27.28, 25.22, 22.40, 18.37.

2-(2-((2-(4-(2-isonicotinoylhydrazinyl)phenoxy)-3-(2-(3,3,5-trimethyl-1-(5-carboxypentyl)-2H-indol-2-ylidene]ethylidene]-1-cyclohexen-1-yl]vinyl]-3,3,5-trimethyl-1-(5-carboxypentyl)-3H-indolium bromide (**Z3**). MS(ESI) m/z: 916.50 $[M-Br]^+$; ^{1}H NMR (600 MHz, CD_3OD) δ 8.73 (s, 2H), 8.32 (s, 1H), 7.89 (d, J=13.3 Hz, 5H), 7.34-7.04 (m, 7H), 6.12 (d, J=14.0 Hz, 2H), 4.05 (s, 4H), 2.73 (s, 4H), 2.34 (s, 6H), 2.15 (s, 4H), 2.10-1.98 (m, 3H), 1.77 (s, 4H), 1.64 (s, 5H), 1.42 (s, 5H), 1.32 (s, 10H), 1.22-1.09 (m, 2H); ^{13}C NMR (101 MHz, CD_3OD) δ 173.25, 164.51, 163.99, 163.12, 151.10, 150.96, 142.64, 142.37, 141.42, 136.59, 131.46, 130.21, 129.85, 124.00, 123.21, 122.44, 116.41, 111.80, 100.96, 66.87, 50.52, 50.18, 49.64, 49.43, 49.21, 49.00, 48.79, 48.57, 48.36, 45.11, 38.63, 28.33, 28.17, 27.85, 27.19, 25.21, 22.41, 21.34, 21.28, 15.44.

Sodium, 2-(2-((2-(4-(2-isonicotinoylhydrazinyl)phenoxy)-3-(2-(3,3-dimethyl-1-(4-sulfonylbutyl)-2H-4,5-benz[e]indol-2-ylidene)ethylidene)-1-cyclohexen-1-yl)vinyl)-3,3-dimethyl-4,5-benz[e]indol-1-yl)butane-1-sulfonate (**Z4**). MS (ESI) m/z: 1054.39 $[M+H]^+$; ^{1}H NMR (600 MHz, DMSO-d_6) δ 8.38 (s, 1H), 8.36 (s, 1H), 8.30 (s, 1H), 8.29 (s, 1H), 8.10 (s, 1H), 8.08 (d, J=5.3 Hz, 2H), 8.06 (s, 1H), 7.82 (d, J=8.8 Hz, 2H), 7.65 (t, J=7.5 Hz, 2H), 7.52 (t, J=7.4 Hz, 2H), 6.43 (s, 1H), 6.40 (s, 1H), 4.41-4.30 (m, 4H), 2.77 (s, 4H), 2.56-2.51 (m, 4H), 1.95 (s, 11H), 1.92-1.84 (m, 6H), 1.79 (dd, J=14.6, 7.3 Hz, 4H); ^{13}C NMR (151 MHz, CD_3OD) δ 175.36, 174.81, 151.07, 150.43, 144.51, 142.24, 141.96, 141.01, 140.93, 135.19, 134.93, 133.47, 133.30, 131.89,

131.10, 129.33, 129.22, 128.78, 128.16, 126.18, 123.39, 123.18, 123.13, 112.27, 102.00, 52.37, 52.01, 51.79, 49.85, 49.64, 49.43, 49.21, 49.00, 48.79, 48.57, 48.36, 45.25, 27.92, 27.57, 27.35, 23.59, 22.12.

Sodium, 2-(2-((2-(4-(2-isonicotinoylhydrazinyl)phenoxy)-3-(2-(3,3-dimethyl-5-methoxy-1-(4-sulfonylbutyl)-2H-indol-2-ylidene)ethylidene)-1-cyclohexen-1-yl) vinyl)-3,3-dimethylindol-1-yl) butane-1-sulfonate (**Z5**). MS(ESI) m/z: 992.40 $[M-Na+2H]^+$; ^1H NMR (600 MHz, DMSO-d_6) δ 8.72 (d, J=6.0 Hz, 2H), 8.42 (s, 1H), 7.79 (dd, J=4.6, 1.5 Hz, 2H), 7.76 (d, J=8.7 Hz, 2H), 7.68 (s, 1H), 7.66 (s, 1H), 7.28 (s, 1H), 7.27 (s, 1H), 7.23 (d, J=8.3 Hz, 2H), 7.13 (d, J=2.4 Hz, 2H), 6.87 (d, J=2.4 Hz, 1H), 6.86 (d, J=2.4 Hz, 1H), 6.14 (s, 1H), 6.11 (s, 1H), 4.10-4.03 (m, 4H), 3.70 (s, 6H), 2.68 (s, 4H), 1.94-1.88 (m, 2H), 1.71 (dt, J=14.4, 7.2 Hz, 5H), 1.65 (dd, J=14.7, 7.6 Hz, 5H), 1.61 (s, 1H), 1.23 (s, 10H), 1.22-1.17 (m, 4H); ^{13}C NMR (101 MHz, CD_3OD) δ 173.14, 172.67, 159.95, 159.72, 151.11, 144.37, 144.20, 141.75, 137.11, 137.06, 131.45, 127.41, 123.19, 122.27, 116.43, 114.95, 114.78, 113.08, 112.82, 110.01, 109.94, 102.03, 100.93, 65.22, 56.46, 56.40, 51.81, 50.75, 50.41, 45.17, 45.02, 28.34, 28.19, 27.35, 23.59.

Sodium, 2-(2-((2-(4-(2-isonicotinoylhydrazinyl)phenoxy)-3-(2-(3,3,5-trimethyl-1-(4-sulfonylbutyl)-2H-indol-2-ylidene)ethylidene)-1-cyclohexen-1-yl)vinyl)-3,3,5-trimethylindol-1-yl)butane-1-sulfonate (**Z6**). MS(ESI) m/z: 982.4 $[M+H]^+$; ^1H NMR (600 MHz, DMSO-d_6) δ 8.72 (d, J=5.7 Hz, 2H), 8.41 (s, 1H), 7.80-7.76 (m, 3H), 7.75 (s, 1H), 7.71 (s, 1H), 7.69 (s, 1H), 7.26 (s, 2H), 7.23 (dd, J=7.9, 4.1 Hz, 4H), 7.12 (s, 1H), 7.11 (s, 1H), 6.17 (s, 1H), 6.15 (s, 1H), 4.10-4.03 (m, 4H), 2.69 (s, 4H), 2.26 (s, 6H), 1.90 (d, J=4.8 Hz, 2H), 1.74-1.67 (m, 5H), 1.64 (dd, J=14.1, 7.2 Hz, 5H), 1.60 (s, 1H), 1.21 (s, 10H), 1.20-1.15 (m, 4H); ^{13}C NMR (101 MHz, DMSO-d_6) δ 171.10, 161.48, 161.45, 160.89, 150.25, 148.55, 141.09, 140.38, 140.02, 139.89, 134.48, 129.63, 128.88, 128.38, 122.97, 121.64, 120.88, 115.04, 111.07, 100.26, 50.69, 48.45, 43.61, 27.51, 27.20, 26.07, 23.72, 22.45, 20.86, 20.75.

5-Bromo-2-(2-((2-(4-(2-isonicotinoylhydrazinyl)phenoxy)-3-(2-(5-bromo-3,3-dimethyl-1-(5-carboxypentyl)-2H-indol-2-ylidene)ethylidene)-1-cyclohexen-1-yl) vinyl)-3,3-dimethyl-1-(5-carboxypentyl)-3H-indolium bromide (**Z7**). MS(ESI) m/z: 1044.29 $[M-Br]^+$; ^1H NMR (600 MHz, CD_3OD) δ 8.73 (d, J=5.1 Hz, 2H), 8.32 (s, 1H), 7.94 (s, 1H), 7.92-7.89 (m, 3H), 7.88 (d, J=5.1 Hz, 2H), 7.55 (s, 2H), 7.49 (s, 1H), 7.48 (s, 1H), 7.22 (s, 1H), 7.20 (s, 1H), 7.19 (s, 1H), 7.18 (s, 1H), 6.18 (s, 1H), 6.16 (s, 1H), 4.06 (t, J=7.2 Hz, 4H), 2.75 (t, J=5.6 Hz, 4H), 2.14 (t, J=7.3 Hz, 4H), 2.07-2.02 (m, 2H), 1.76 (dt, J=14.6, 7.3 Hz, 4H), 1.68-1.59 (m,5H), 1.45-1.38 (m, 5H), 1.34 (s, 11H), 1.32 (s, 1H); ^{13}C NMR (101 MHz, CD_3OD) δ 182.37, 173.22, 164.89, 163.12, 151.10, 150.81, 144.64, 143.11, 142.90, 142.56, 132.77, 131.51, 130.04, 126.81, 123.81, 123.20,119.04, 116.45, 113.73, 101.66, 101.39, 66.89, 50.37, 45.28, 38.80, 28.04, 27.83, 27.23, 25.21, 22.34, 15.43.

Sodium, 2-(2-((2-(4-(2-isonicotinoylhydrazinyl)phenoxy)-3-(2-(3,3-dimethyl-1-(4-sulfonylbutyl)-2H-indol-2-ylidene) ethylidene]-1-cyclohexen-1-yl)vinyl)-3,3-dimethyl-4,5-benz[e]indol-1-yl)butane-1-sulfonate (**Z8**). MS(ESI) m/z: 1004.37 $[M+H]^+$; ^1H NMR (400 MHz, CD_3OD) δ 8.76 (s, 2H), 8.45-8.33 (m, 1H), 8.14 (d, J=8.9 Hz, 2H), 7.99 (q, J=10.4 Hz, 5H), 7.92 (s, 2H), 7.72-7.55 (m, 2H), 7.49 (d, J=7.5 Hz, 1H), 7.39 (d, J=5.3 Hz, 2H), 7.32 (d, J=8.5 Hz, 3H), 7.21 (dd, J=15.8, 8.2 Hz, 1H), 6.41-6.25 (m, 1H), 6.22 (d, J=14.0 Hz, 1H), 4.31 (s, 2H), 4.15 (s, 2H), 3.01-2.87 (m, 4H), 2.84 (s, 4H), 2.18-1.87 (m, 10H), 1.74-1.60 (m, 6H), 1.44-1.30 (m, 6H); ^{13}C NMR (101 MHz, CD_3OD) δ 175.70, 172.78, 164.47, 164.21, 163.17, 151.10, 143.65, 143.49, 143.00, 142.87, 142.42, 142.27, 142.13, 140.85, 135.34, 133.48, 133.34, 131.86, 131.53, 131.08, 129.88, 129.75, 129.20, 128.77, 126.22, 126.04, 125.86, 123.33, 123.21, 123.14, 116.52, 112.28, 112.13, 111.84, 101.58, 101.37, 100.97, 100.76, 66.87, 52.28, 52.08, 51.84, 50.26, 50.04, 49.64, 49.43, 49.21, 49.00, 48.79, 48.57, 48.36, 45.24, 44.75, 28.26, 28.20, 27.81, 27.54, 27.22, 27.17, 25.22, 23.58, 22.42.

2-(2-((2-(4-(2-Isonicotinoylhydrazinyl)phenoxy)-3-(2-(5-bromo-3,3-dimethyl-1-(5-carboxypentyl)-2H-indol-2-ylidene)ethylidene)-1-cyclohexen-1-yl)vinyl)-3,3-dimethyl-1-(5-carboxypentyl)-3H-indolium bromide (**Z9**). MS(ESI) m/z: 966.37 $[M-Br]^+$; ^1H NMR (600 MHz, CD_3OD) δ 8.01 (d, J=14.5 Hz, 2H), 7.90 (d, J=8.7 Hz, 1H), 7.87 (d, J=4.8 Hz, 2H), 7.80 (d, J=13.9 Hz, 1H), 7.47 (d, J=1.8 Hz, 1H), 7.43 (dd, J=8.4, 1.8 Hz, 1H), 7.38 (dd, J=14.6, 7.4 Hz, 2H), 7.34 (t, J=7.5 Hz, 1H), 7.23 (t, J=6.3 Hz, 1H), 7.20 (d, J=8.7Hz, 2H), 7.08 (d, J=8.5 Hz, 1H), 6.28 (d, J=14.5 Hz, 1H), 6.03 (d, J=13.9 Hz, 1H), 4.15 (t, J=7.4 Hz, 2H), 3.97 (t, J=7.3 Hz, 2H), 2.78-2.70 (m, 4H), 2.14 (td, J=7.4, 3.1 Hz, 4H), 2.07-2.00 (m, 2H), 1.76 (ddt, J=29.6, 14.2, 7.2 Hz, 4H), 1.63 (dq, J=14.8, 7.4 Hz, 4H), 1.42 (dt, J=16.6, 8.0 Hz, 4H), 1.36-1.29 (m, 12H); ^{13}C NMR (101 MHz, CD_3OD) δ 176.23, 171.44, 171.03, 151.09, 151.01, 147.26, 145.41, 144.28, 143.60, 143.54, 143.35, 143.28, 143.25, 143.16, 143.10, 142.88, 142.58, 142.43, 142.31, 132.65, 131.51, 130.07, 128.82, 128.10, 127.46, 126.77, 123.64, 123.49, 123.35, 123.24, 118.17, 116.41, 113.17, 113.12, 104.40, 100.89, 51.25, 50.61, 50.02, 45.77, 44.96, 38.60, 38.56, 28.49, 28.35, 28.18, 28.01, 27.93, 27.86, 27.81, 27.37, 27.30, 27.18, 27.13, 22.07.

Sodium, 2-(2-((2-(4-(2-isonicotinoylhydrazinyl)phenoxy)-3-(2-(3,3,5-trimethyl-1-(4-sulfonylbutyl)-2H-indol-2-ylidene)ethylidene)-1-cyclohexen-1-yl]vinyl]-3,3-dimethyl-4,5-benz[e]indol-1-yl)butane-1-sulfonate (**Z10**). MS (ESI) m/z: 1040.37 $[M+Na]^+$; ^1H NMR (400 MHz, CD_3OD) δ 8.74 (d, J = 5.7 Hz, 2H), 8.41 (s, 1H), 8.14-8.00 (m, 2H), 8.02-7.86 (m, 6H), 7.65-7.49 (m, 2H), 7.49-7.36 (m, 1H), 7.27 (d, J = 8.6 Hz, 2H), 7.20 (t, J = 8.5Hz, 3H), 6.22 (dd, J = 14.3, 4.8 Hz, 2H), 4.22 (d, J = 6.7 Hz, 2H), 4.13 (d, J = 6.4 Hz, 2H), 2.90 (d, J = 5.6 Hz, 4H), 2.79 (d, J = 5.7 Hz, 4H), 2.37 (s, 3H), 2.14-1.85 (m, 10H), 1.65 (s, 6H), 1.35 (s, 6H); ^3C NMR (101 MHz, CD_3OD) δ 174.42, 173.73, 164.48, 164.03, 163.15, 151.09, 151.02, 142.92, 142.75, 142.62, 142.48, 142.36, 141.59, 141.37, 141.30, 141.06, 136.83, 136.55, 134.71, 133.24, 131.73, 131.51, 131.05,130.28, 129.84, 129.30, 128.63, 125.89, 124.01, 123.19, 122.99, 122.87, 122.70, 116.51, 112.07, 112.03, 101.60,100.46, 52.07, 51.91, 51.82, 51.79, 50.33, 50.17, 49.64, 49.43, 49.21, 49.00, 48.79, 48.57, 48.36, 45.04, 44.94, 28.16, 27.85, 27.43, 27.30, 27.24, 25.25, 25.21, 23.58, 22.43, 21.29.

Conflicts of interest: None declared.

Acknowledgments: This study was financially supported by the Innovative Talent Support Program of Higher Education in Liaoning province (No. 46).

References

Aggarwal R, Ryan CJ (2011) Castration-resistant prostate cancer: targeted therapies and individualized treatment. The oncologist 16: 264–275.

Flam V, Zhao H, Peehl DM (2010) Targeting monoamine oxidase A in advanced prostate cancer. J Cancer Res Clin 136: 1761–1771.

Heidegger I, Massoner P, Eder IE, Pircher A, Pichler R, Aigner F, Bektic J, Horninger W, Klocker H (2013) Novel therapeutic approaches for the treatment of castration-resistant prostate cancer. J Steroid Biochem Mol Biol 138: 248–256.

Henary M, Pannu V, Owens EA, Aneja R (2012) Near infrared active heptacyanine dyes with unique cancer-imaging and cytotoxic properties. Bioorg Med Chem Lett 22: 1242–1246.

Hong G, Antaris AL, Dai H (2017) Near-infrared fluorophores for biomedical imaging. Nature Biomed Engin 1: 0010.

Jolene O, Michael RH, Mahmoud AP (2015) Inhibition of excessive monoamine oxidase A/B activity protects against stress-induced neuronal death in huntington disease. Mol Neurobiol 52: 1850–1861.

Kgatle MM, Kalla AA, Islam, MM, Sathekge M, Moorad R (2016) Prostate cancer: epigenetic alterations, risk factors, and therapy. Prostate Cancer 2016: P5653862.

Khemthongcharoen N, Jolivot R, Rattanavarin S, Piyawattanametha W (2013) Advances in imaging probes and optical microendoscopic imaging techniques for early in vivo cancer assessment. Adv Drug Deliver Rev 74: 53–74.

Li PC, Siddiqi IN, Mottok A, Loo EY, Wu CH, Cozen W, Steidl C, Shih JC (2017) Monoamine oxidase A is highly expressed in classical Hodgkin lymphoma. J Pathol 243: 220–229.

Liao CP, Lin TP, Li PC, Geary LA, Chen K, Vaikari VP, Wu JB, Lin CH, Gross ME, Shih JC (2018) Loss of MAOA in epithelia inhibits adenocarcinoma development, cell proliferation and cancer stem cells in prostate. Oncogene 37: 5175–5190.

Liu F, Hu L, Ma Y, Huang B, Xiu Z, Zhang P, Zhou K, Tang X (2017) Increased expression of monoamine oxidase A is associated with epithelial to mesenchymal transition and clinicopathological features in non-small cell lung cancer. Oncol Lett 15: 3245–3251.

Luo S, Tan X, Qi Q, Guo Q, Ran X, Zhang L, Zhang E, Liang Y, Weng L, Zheng H, Cheng T, Su Y, Shi C (2013) A multifunctional heptamethine near-infrared dye for cancer theranosis. Biomaterials 34: 2244–2251.

Luo S, Zhang E, Su Y, Cheng T, Shi C (2011) A review of NIR dyes in cancer targeting and imaging. Biomaterials 32: 7127–7138.

Lv Q, Wang D, Yang Z, Yang J, Zhang R, Yang X, Wang M, Wang Y (2019) Repurposing antitubercular agent isoniazid for treatment of prostate cancer. Biomater Sci 7: 296–306.

Lv Q, Yang X, Wang M, Yang J, Qin Z, Kan Q, Zhang H, Wang Y, Wang D, He Z (2018) Mitochondria-targeted prostate cancer therapy using anear-infrared fluorescence dye-monoamine oxidase A inhibitor conjugate. J Control Release279: 234–242.

Oliveira, PFM, Guidetti B, Chamayou A, André-Barrès C, Madacki J, Korduláková J, Mori G, Orena BS, Chiarelli LR, Pasca MR, Lherbet C, Carayon C, Massou S, Baron M, Baltas M (2017) Mechanochemical synthesis and biological evaluation of novel isoniazid derivatives with potent antitubercular activity. Molecules 22: 1457–1483.

Pahontu E, Ilies DC, Shova S, Oprean C, Păunescu V, Olaru OT, Rădulescu FŞ, Gulea A, RoŞu T, Drăgănescu D (2017) Synthesis, characterization, antimicrobial and antiproliferative activity evaluation of Cu(II), Co(II), Zn(II), Ni(II) and Pt(II) complexes with isoniazid-derived compound. Molecules 22: 650–666.

Peehl DM, Coram M, Khine H, Reese S, Nolley R, Zhao H (2008) The significance of monoamine oxidase-A expression in high grade prostate cancer. J Urology 180: 2206–2211.

Stavridi F, Karapanagiotou EM, Syrigos KN (2010) Targeted therapeutic approaches for hormone-refractory prostate cancer. Cancer Treat Rev 36: 122–130.

Sandi C, Haller J (2015) Stress and the social brain: behavioural effects and neurobiologicalmechanisms. Nat Rev Neurosci 16: 290–304.

Schwartz TL (2013) A neuroscientific update on monoamine oxidase and its inhibitor. CNS Spectrums 18: 22–33.

Sevick-Muraca EM (2012) Translation of near-infrared fluorescence imaging technologies: emerging clinical applications. Annu Rev Med 63: 217–231.

Shih JC, Chen K, Ridd MJ (1999) Monoamine oxidase: from genes to behavior. Annu Rev Neurosci 22: 197–217.

Shi C, Wu JB, Chu G, Chu GC, Li Q, Wang R, Zhang C, Zhang Y, Kim HL, Wang J, Zhau HE, Pan D, Chung LW (2014) Heptamethine carbocyanine dye-mediated near-infrared imaging of canine and human cancers through the HIF-1α/OATPs signaling axis. Oncotarget 5: 10114–10126.

Sun W, Choi J, Cha Y, Koo J (2017) Evaluation of the expression of amine oxidase proteins in breast cancer. Int J Mol Sci 18: 2775–2775.

Tan X, Luo S, Wang D, Su Y, Cheng T, Shi C (2012) A NIR heptamethine dye with intrinsic cancer targeting, imaging and photosensitizing properties. Biomaterials 33: 2230–2239.

True L, Coleman I, Hawley S, Huang CY, Gifford D, Coleman R, Beer TM, Gelmann E, Datta M, Mostaghel E, Knudsen, B, Lange P, Vessella R, Lin D, Hood L, Nelson PS (2006) A molecular correlate to the Gleason grading system for prostate adenocarcinoma. P Natl Acad Sci USA 103: 10991–10996.

Vila-Vicosa D, Victor BI, Ramos J, Machado D, Viveiros M, Switala J, Loewen PC, Leitão R, Martins F, Machuqueiro M (2017) Insights on the mechanism of action of INH-C10 as an antitubercular prodrug. Mol Pharm 14: 4597–4605.

Wang GL, Jiang BH, Rue EA, Semenza GL (1995) Hypoxia-inducible factor 1 is a basic-helix-loop-helix-PAS heterodimer regulated by cellular O_2 tension. Proc Natl Acad Sci USA 92: 5510–5514.

Wu HF, Chen KJ, Shih C (1993) Site-directed mutagenesis of monoamine oxidase A and B: role of cysteines. Mol Pharmacol 43: 888–893.

Wu JB, Lin TP, Gallagher JD, Kushal S, Chung LW, Zhau HE, Olenyuk BZ, Shih JC (2015) Monoamine oxidase A inhibitor-near-infrared dye conjugate reduces prostate tumor growth. J Am Chem Soc 137: 2366–2374.

Wu JB, Shao C, Li X, Li Q, Hu P, Shi C, Li Y, Chen YT, Yin F, Liao CP, Stiles BL, Zhau HE , Shih JC, Chung LW (2014) Monoamine oxidase A mediates prostate tumorigenesis and cancer metastasis. J Clin Invest 124: 2891–2908.

Wu JB, Shao C, Li X, Shi C, Li Q, Hu P, Chen YT, Dou X, Sahu D, Li W, Harada H, Zhang Y, Wang R, Zhau HE, Chung LW (2014) Near-infrared fluorescence imaging of cancer mediated by tumor hypoxia and HIF1alpha/OATPs signaling axis. Biomaterials 35: 8175–8185.

Xiao L, Zhang Y, Yue W, Xie X, Wang JP, Chordia MD, Chung LW, Pan D (2013) Heptamethine cyanine based (64) Cu-PET probe PC-1001 for cancer imaging: synthesis and in vivo evaluation. Nucl Med Biol 40: 351–360.

Xu S, Adisetiyo H, Tamura S, Grande F, Garofalo A, Roy-Burman P, Neamati N (2015) Dual inhibition of survivin and MAOA synergistically impairs growth of PTEN-negative prostate cancer. Br J Cancer 113: 242–251.

Yang X, Shi C, Tong R, Qian W, Zhau HE, Wang R, Zhu G, Cheng J, Yang VW, Cheng T, Henary M, Strekowski L, Chung LW (2010) Near IR heptamethine cyanine dye-mediated cancer imaging. Clin. Cancer Res 16: 2833–2844.

Yang XG, Mou YH, Wang YJ, Wang J, Li YY, Kong RH, Ding M, Wang D, Guo C (2019) Design, Synthesis, and Evaluation of Monoamine Oxidase A Inhibitors–Indocyanine Dyes Conjugates as Targeted Antitumor Agents. Molecules 24: 1400.

Zhao H, Flam V, Peehl, DM (2009) Anti-oncogenic and pro-differentiation effects of clorgyline, a monoamine oxidase A inhibitor, on high grade prostate cancer cells. BMC Med Genomics 2: 55–69.